Phase Transition to an Opaque Plasma in a Sonoluminescing Bubble

Brian Kappus,[1,*] Shahzad Khalid,[1] Avik Chakravarty,[1] and Seth Putterman[1,2]

[1]Department of Physics and Astronomy, University of California, Los Angeles, California 90095, USA

[2]California Nano-Systems Institute , University of California, Los Angeles, California 90095, USA

(Received 30 July 2010; revised manuscript received 26 February 2011; published 8 June 2011)

Time-resolved spectrum measurements of a sonoluminescing Xe bubble reveal a transition from transparency to an opaque Planck blackbody. As the temperature is <10 000 K and the density is below liquid density, the photon scattering length is 10 000 times too large to explain its opacity. We resolve this issue with a model that reduces the ionization potential. According to this model, sonoluminescence originates in a new phase of matter with high ionization. Analysis of line emission from Xe* also yields evidence of phase segregation for this first-order transition inside a bubble.

DOI: 10.1103/PhysRevLett.106.234302 PACS numbers: 78.60.Mq, 43.25.+y

The fundamental blackbody law of radiation results from Planck's realization that in thermal equilibrium photons have a model independent spectrum. So a key criterion underlying blackbody emission is that photons and matter are in equilibrium, which means that a blackbody is opaque. An explanation of the observation that picosecond flashes emitted from a radially pulsating, micron-sized bubble follow Planck's law is a key unknown of sonoluminescence [1]. Modeling with simple theories of plasma physics indicates that the bubble's radius is 5 orders of magnitude too small to admit collisions between photons and matter. For instance, a xenon bubble in water that is driven to pulsate by the action of a 40 kHz standing sound wave radiates as an 8000 K ideal Planck blackbody when it reaches a minimum radius of 0.7 μm [1]. Opacity is due to the scattering of light by unbound electrons [2,3]. As the temperature T is small compared to the ionization potential ($\chi_0 = 180.000$ K) of xenon, the Boltzmann factor of statistical mechanics leads to a degree of ionization ($x \sim 1.5 \times 10^{-4}$) that is too small to explain the observed opacity by several orders of magnitude. For this reason various explanations of the sonoluminescing Planck spectrum invoke an off equilibrium hot inner core [4–7] while the majority of theories insist that a sonoluminescing bubble is transparent [8–12].

An insight into this conundrum comes from measurements of the opacity and electron density in sonoluminescing sulfuric acid bubbles. These bubbles emit as 7000 K blackbodies with a radius of 4 μm [13]. In order to be opaque at this radius, the electron density needs to be $>10^{21}/\text{cm}^3$. Analysis of line spectra supports this value [6]. Statistical mechanics in the dilute gas limit once again predicts a much lower level of ionization.

We propose that this conundrum is explained by collective processes that dramatically increase the degree of ionization by strongly lowering the ionization potential. Here we present a qualitative model for the reduction of χ in a sonoluminescence (SL) microplasma. This model is then tested with new experimental measurements of the transition from transparent to blackbody behavior which occurs during a single flash of SL from a bubble that has a low atomic density.

A picture of how collective processes could increase ionization is described by qualitatively including the effects of electrostatic screening and quantum hybridization of the electronic energy levels. These corrections to χ_0 arise because Debye screening reduces the distance an electron must move from an atom to be liberated to $\delta_D = \sqrt{kT/8\pi n_e e^2}$ ([2], p. 217), thus reducing the ionization potential by e^2/δ_D. Also, in dense gases the ionization potential is lowered to the binding energy of an excited atom whose radius equals the interatomic spacing ([2], p. 199). With these effects, we find that

$$\chi \approx \chi_0(1 - 2\gamma a_B n_0^{1/3}) - e^2/\delta_D, \tag{1}$$

where a_B is the Bohr radius (0.53 Å) and e the fundamental unit of charge. For a hydrogen atom $\gamma = 1$. Experiments on photon induced conductivity in cold xenon at high pressure [14] indicate $\gamma = 1.78$. The electron's density is $n_e = xn_0$ so that x is the degree of ionization.

Ionization is controlled by the Boltzmann factor as described by Saha:

$$\frac{x^2}{1-x} = \frac{2g_1}{n_0\lambda^3}\exp\{-\chi/kT\}, \tag{2}$$

where g_1 is the effective degeneracy of the electronic states of the ion (at 8000 K g_1 is 2.6 and at 10 000 K g_1 is 2.9), $\lambda = h/\sqrt{2\pi m_e kT}$ is the electron thermal de Broglie wavelength (it is 8.4 Å at 8000 K and 7.5 Å at 10 000 K). Using the tabulated value of the xenon's ionization potential ($\chi = \chi_0 = 12.1$ eV) with the conditions in the 40 kHz SL bubble (temperature 8000 K, 0.7 μm collapse radius indicating $n_0 = 10^{22}$ Xe/cm^3), Saha's equation predicts the previously mentioned low degree of ionization, $x = 1.5 \times 10^{-4}$ (and corresponding large value of ℓ). In order to be opaque the degree of ionization inside this bubble needs to be about 1000 times larger. Using the corrected ionization potential (1) we can now identify a mechanism to generate a dramatically different state of plasma in a sonoluminescing bubble that is highly ionized.

The corrected ionization potential (1) and Saha's equation (2) are coupled because the Debye screening length itself depends upon the electron density $n_e = xn_0$. Therefore, when using the corrected ionization potential one must seek a self-consistent solution to (1) and (2) [15]. Figure 1 shows that such a solution has two branches when the density is lower than a critical value of $n_0 = n_c \approx 3 \times 10^{21}/\mathrm{cm}^3$. Sonoluminescence from a single bubble driven at 40 kHz exists at densities above this value, and according to this theory the xenon atoms in the bubble are all at least singly ionized. A similar analysis [15] indicates that a sonoluminescing hydrogen bubble at 6000 K ($n_0 = 1.35 \times 10^{22}$ H_2 molecules/cm^3) has reached an opacity which qualifies it as having reached a state of black hydrogen, which has been sought after in many other experiments [16–18].

An experimental test of this overarching theory of sonoluminescence requires probing bubbles with densities below n_c. At these lower densities Eqs. (1) and (2) admit two solutions (dot and shaded bar for given density in Fig. 1) leading to two plasma phases with very distinct properties: one with low ionization and one with high ionization are predicted to exist at a given temperature T. The lower x solution is stable, but the higher x solution (dashed line) is an unstable maximum of the free energy [15]. Above this point our theory only admits a decreasing free energy with higher x. If a portion of the bubble's interior reaches the upper degree of ionization through a fluctuation, then x will continue to increase until a stable limit is achieved. This is suggestive of a phase-transition-like behavior of the plasma properties. An important feature missing from this model is the mechanism that ultimately limits x in the highly ionized phase. The existence of a phase transition in this region is unexpected because the overall atomic density is so low that there is no overlap between the electron orbitals of the neutral xenon atoms.

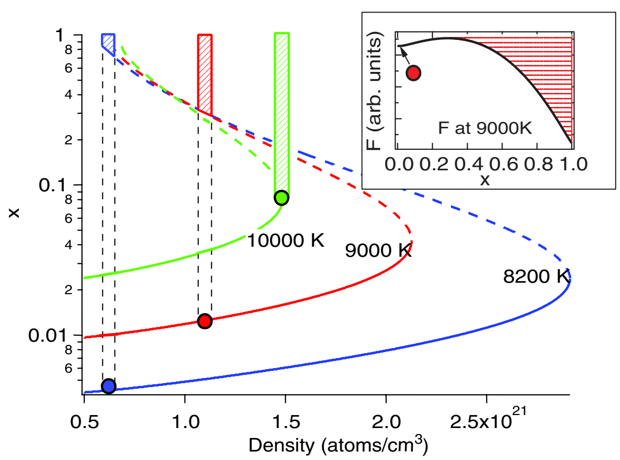

FIG. 1 (color online). Solutions to Eqs. (1) and (2) for the degree of ionization x as a function density of Xe atoms for various temperatures. The lower branch solid lines correspond to a minimum of the free energy, and the upper branch dashed lines correspond to a maximum as indicated by the inset which displays a plot of the free energy as a function of x for point 6. Note that the density $\sim 10^{22}/\mathrm{cm}^3$ of single bubble sonoluminescence at 40 kHz lies to the right of these curves.

In order to compare SL to this theory in the dilute gas limit we have measured sonoluminescence in a regime where the implosion is weaker and the flash duration is longer. This is achieved when a xenon bubble is trapped in a column of phosphoric acid which is vibrating vertically at 40 Hz [19–21]. To measure bubble radius as a function of time, a streak camera was constructed with two Nikon camera lenses (50 and 105 mm) and a two-sided mirror attached to a Dremel tool. Streak images were captured using a CCD camera (Hamamatsu C4742-98-24ER) placed 20 cm from the rotating mirror and backlighting was provided by an infrared diode laser (Powertechnology LDCU12/7108). A time-resolved spectrum utilized an intensified CCD (Princeton Instruments ICCD-MAX) attached to a grating spectrometer (300i, Acton Research) which observed the SL through a broadband optical fiber placed at 5 cm. The ICCD was triggered by a photomultiplier tube (Hamamatsu H5783-03) with an adjustable delay provided by a delay box (SRS DG535) [15].

For this system the flash width is ~ 1.0 μs, the velocity of collapse is much less than the speed of sound in the xenon gas, and the maximum density, which is achieved at $R_c \sim 50$ μm, is reduced by a factor of 7 (compared to 40 kHz SL) to $n_0 = 1.5 \times 10^{21}$ Xe atoms/cm^3. Even for these weak implosions, time-resolved spectra (Fig. 2) indicate that an equilibrium blackbody forms inside the bubble as its radius approaches R_c. Although the low frequency bubbles have a larger radius, the calculated $\ell \sim 10^4 R_c$, using χ_0, is still inconsistent with their opacity.

At any given time during the flash a measured spectrum is used to calculate two different radii (see inset of Fig. 2). By fitting Planck's law to the broadband portion of the spectrum we obtain the radius R_{bb} and temperature T of an ideal spherical blackbody with the identical irradiance. In addition to the continuous part of the spectrum, one observes, during the early and latter intervals of the flash, a line at 823 nm which is due to a strongly coupled downward transition to the first excited state: Xe* at 8.3 eV [22]. The second spectral radius R^* is determined by a blackbody fit, with the same temperature as the spectral continuum, to the peak of the line at 823 nm. The radius of the bubble wall R is obtained from backlit streak images of the pulsating bubble. Figure 3 presents a plot of T, R^*, R_{bb}, and R as a function of time during the flash.

The existence of the 400 ns interval centered around R_c where R^*, R_{bb}, and R are equal (Fig. 3) is strong evidence for the formation of a blackbody in these weakly collapsing bubbles. The high degree of ionization required for the

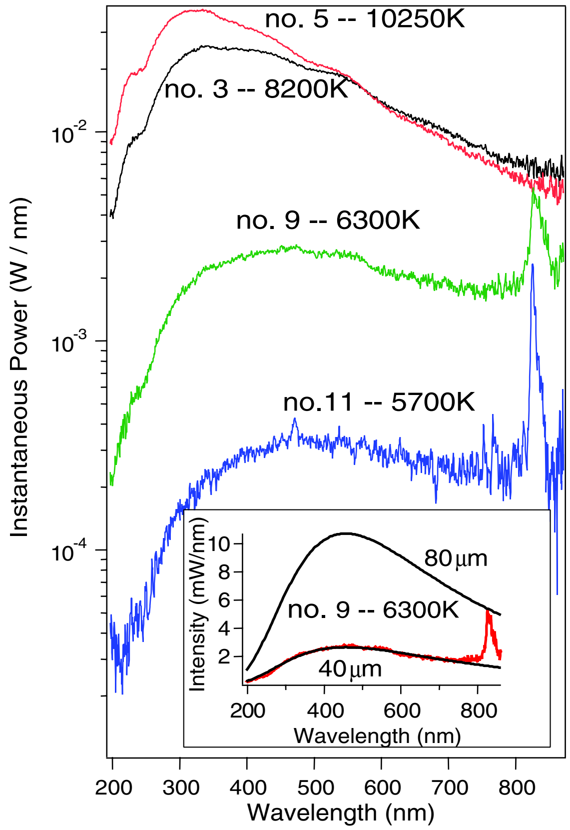

FIG. 2 (color online). Time-resolved spectra for a sonoluminescing xenon bubble pulsating in phosphoric acid at 40 Hz (see the section on methods). The time between successive spectra is 100 ns and spectrum no. 5 coincides with the minimum radius and occurs 500 ns into the flash. The spectra have contributions from a thermal continuum as well as a line at 823 nm. The quality of the blackbody fit to the thermal portion of the spectrum is equally good for the data near R_c as well as the data where the 823 line is prominent. Each acquisition is 10 ns in duration, and the graph is the average of 100 acquisitions in each of 4 different grating positions. The inset shows the best blackbody fits to the continuum and the top of the 823 nm spectral line at point no. 9 which occurs 400 ns after the minimum radius when the temperature is 6200 K. The blackbody fits differ only in the radius of the region of emission, $R_{bb} = 40\ \mu$m and $R^* = 80\ \mu$m.

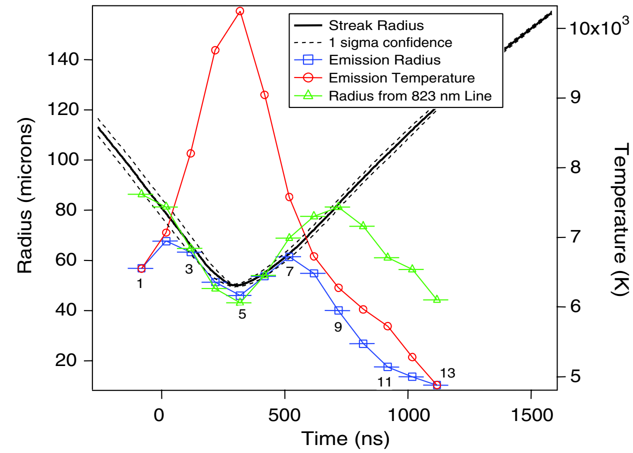

FIG. 3 (color online). Radii and blackbody temperature for a sonoluminescing bubble at 40 Hz. The radius of the wall of the bubble R is obtained with a backlit streak image and is shown in black. The blackbody temperature and radius R_{bb} obtained from fitting the thermal portion of the spectra in Fig. 2 is shown in red and blue, respectively. The radius R^* of the blackbody whose spectrum passes through the peak of the emission at 823 nm at the temperature determined by the red line is shown in green. Horizontal error bars represent the uncertainty in synchronizing spectrums and streak images in time.

formation of an opaque emitter is now interpreted in terms of a transition to a new plasma phase, as outlined in Fig. 1. Furthermore, the manner in which these radii diverge about 300 ns before (and after) R_c is reached is evidence for two segregated regions inside the sonoluminescing bubble. These regions are characterized by their differing degrees of ionization. The region with a radius R_{bb} is an opaque plasma phase with a high degree of ionization. The second region has a low degree of ionization and is transparent. This outer region is the source of line emission, and fills the portion of the bubble that is not radiating as a blackbody. So even when R_{bb} has shrunk to less than $\frac{1}{2}R$, the radius R^* characteristic of line emission remains equal to R for points 1, 2, 8, and 9 marked on Fig. 2. As a blackbody is a maximally efficient emitter, the peak of an emission line cannot exceed the height of a blackbody spectrum at the same temperature for the same size emitter ([2], p. 247). The peak line emission can be less than blackbody emission at the same temperature, but here the strength of the line at 823 nm causes it to meet the blackbody curve whose radiance is limited by the size of the bubble. A cooler outer region can also be ruled out by this analysis as this interpretation leads to the unphysical conclusion that $R^* > R$. Therefore, we conclude that the two segregated regions have the same temperature and are the physical realization of the two branches of the solution to Eqs. (1) and (2) with dramatically different degrees of ionization determining their transparency and opacity.

The importance of the upper branch solution in these shake bubble experiments may be demonstrated by analysis at the moment where the bubble first becomes opaque (point 3 in Fig. 3). At this point, its radius decreases through 65 μm where the spectral temperature is 8200 K and the density is $6.5 \times 10^{20}/\mathrm{cm}^3$. The degree of ionization according to the uncorrected Saha equation is $x \approx 7.2 \times 10^{-4}$. For such a small degree of ionization, $\ell/R \sim 10^4$, when a 300 nm photon is absorbed during a collision between a free electron and a neutral atom ([2], p. 283) with a cross section of ($3.1 \times 10^{-16}\ \mathrm{cm}^2$) [23]. Yet we observe a blackbody spectrum to within 5% which corresponds to $\pi\ell/R = 1$.

The blackbody nature of point 3 is explained by the highly ionized solution on the upper branch of Fig. 1. In this case Eq. (1) includes an additional correction of

$-\alpha e^2/2\delta_D^4$ to polarization of the newly formed xenon ion (the polarizability is $\alpha = 4$ Å^3 [24]), which is similar to corrections used for metallic plasmas [25]. The degree of ionization above the upper branch is greater than 70% and, therefore, $\pi\ell/R < 1/2$ and an opaque response is realized. For such a high degree of ionization, ℓ is dominated by the inverse process whereby an electron scatters off of a positively charged ion to make light ([2], p. 259). The degree of ionization at point 3 in the lower branch is $x = 4 \times 10^{-3}$, which would still be transparent with $\pi\ell/R = 10^3$. The contribution of photodissociation of $Xe_2{}^+$ molecules to the opacity is small [15].

Use of the Debye length to screen the potential felt by a freed electron involves the use of a continuum theory when the screening length is smaller than the average interion spacing,$a = (3/4\pi x n_0)^{1/3}$. Brush, Sahlin, and Teller have simulated the statistical mechanics of a plasma where one species of charge moves in a fixed uniform neutralizing background [26]. They find that when $\delta_D/a \sim 1.8$, a continuum description in terms of a Debye screening length is correct within the accuracy ($\sim 5\%$) of their calculations. When the Landau parameter $\Gamma \equiv e^2/akT$ is unity (which in our case corresponds to $\delta_D/a = 1/2.5$ at point 3 with $x = 1$), the free energy calculated from the continuum approach is off by about 25%. It remains to be seen whether the statistical mechanical description of a gas where both ions and electrons are free to seek equilibrium will support the magnitude of ionization potential reduction required by experiment, or whether one needs to bring in a new correlation.

Sonoluminescing bubbles with a blackbody spectrum have now been experimentally observed with densities ranging from $7 \times 10^{20}/\mathrm{cm}^3$ for xenon at 8200 K to $1.35 \times 10^{22}/\mathrm{cm}^3$ for hydrogen at about 6000 K. Our observations are reminiscent of investigations of Mott transitions [27] and conducting-insulating transitions [28–30] under conditions where electron shells in plasmas have been crushed together. In contrast, the SL phase transition is effective even as the dilute gas limit is approached. For the micron-sized hydrogen bubble which can be driven to flash 40 000 times per second, the electron density required to explain its 6000 K blackbody spectrum implies a Fermi degeneracy temperature T_F greater than 6000 K ($T_F \sim 24\,000$ if $x = 1$). Sonoluminescing bubbles may provide a route to the study of quantum degenerate and quantum screened plasmas.

This project is supported by DARPA and generous contributions from the Stephanie and Elwood Norris Foundation. We thank Carlos Camara for valuable advice regarding all aspects of the project. We thank David DeMille, E. L. Wright, Michael Desjarlais, and Keith Weninger for valuable discussions.

*To whom correspondence should be addressed.
kappus@physics.ucla.edu

[1] G. Vazquez *et al.*, Opt. Lett. **26**, 575 (2001).
[2] Y. B. Zel'dovich and Y. P. Raæizer, *Physics of Shock Waves and High-Temperature Hydrodynamic Phenomena* (Dover, Mineola, NY, 2002), p. xxvii.
[3] H. R. Griem, *Principles of Plasma Spectroscopy* (Cambridge University Press, Cambridge, England, 1997), p. xix.
[4] D. J. Flannigan and K. S. Suslick, Nature (London) **434**, 52 (2005).
[5] H. X. Xu and K. S. Suslick, Phys. Rev. Lett. **104**, 244301 (2010).
[6] D. J. Flannigan and K. S. Suslick, Nature Phys. **6**, 598 (2010).
[7] G. Vazquez *et al.*, Phys. Rev. Lett. **88**, 197402 (2002).
[8] S. Hilgenfeldt, S. Grossmann, and D. Lohse, Nature (London) **398**, 402 (1999).
[9] W. K. Tse and P. T. Leung, Phys. Rev. E **73**, 056302 (2006).
[10] P. D. S. Burnett *et al.*, J. Quant. Spectrosc. Radiat. Transfer **71**, 215 (2001).
[11] C. C. Wu and P. H. Roberts, Proc. R. Soc. A **445**, 323 (1994).
[12] D. Hammer and L. Frommhold, J. Mod. Opt. **48**, 239 (2001).
[13] S. D. Hopkins *et al.*, Phys. Rev. Lett. **95**, 254301 (2005).
[14] K. Syassen, Phys. Rev. B **25**, 6548 (1982).
[15] See supplemental material at http://link.aps.org/supplemental/10.1103/PhysRevLett.106.234302 for additional information.
[16] P. Loubeyre, F. Occelli, and R. LeToullec, Nature (London) **416**, 613 (2002).
[17] P. M. Celliers *et al.*, Phys. Rev. Lett. **84**, 5564 (2000).
[18] H. K. Mao and R. J. Hemley, Science **244**, 1462 (1989).
[19] C. K. Su *et al.*, Phys. Fluids **15**, 1457 (2003).
[20] A. Chakravarty *et al.*, Phys. Rev. E **69**, 066317 (2004).
[21] R. Urteaga, P. L. Garcia-Martinez, and F. J. Bonetto, Phys. Rev. E **79**, 016306 (2009).
[22] C. J. Humphrey and E. Paul, J. Opt. Soc. Am. **60**, 1302 (1970).
[23] A. W. Yau, R. P. Mceachran, and A. D. Stauffer, J. Phys. B **13**, 377 (1980).
[24] A. Zangwill and P. Soven, Phys. Rev. A **21**, 1561 (1980).
[25] R. Redmer, Phys. Rev. E **59**, 1073 (1999).
[26] S. G. Brush, H. L. Sahlin, and E. Teller, J. Chem. Phys. **45**, 2102 (1966).
[27] D. Kremp *et al.*, *Quantum Statistics of Nonideal Plasmas* (Springer, Berlin, 2005), p. xi.
[28] V. E. Fortov *et al.*, J. Exp. Theor. Phys. **97**, 259 (2003).
[29] S. Kuhlbrodt *et al.*, Contrib. Plasma Phys. **45**, 61 (2005).
[30] W. Ebeling *et al.*, Physica (Amsterdam) **150A**, 159 (1988).